

Gas separation by kinked single-walled carbon nanotubes: Molecular dynamics simulations

ZhongQiang Zhang, HongWu Zhang,* YongGang Zheng, Lei Wang, and JinBao Wang

State Key Laboratory of Structural Analysis for Industrial Equipment, Department of Engineering Mechanics, Faculty of Vehicle Engineering and Mechanics, Dalian University of Technology, Dalian 116024, People's Republic of China

(Received 10 May 2008; published 23 July 2008)

In this paper, a kink model for gas separation is presented. Transport of pure nitrogen, oxygen, and their mixture in single-walled carbon nanotubes (SWCNTs) with a kink formed by bending is studied using molecular dynamics simulations. The results show that a nanotube with a specified kink results in transport resistance to nitrogen, while allowing oxygen to pass even though the two gases have very similar molecular sizes. The permeability decreases while the selectivity increases with increasing the bending angle of SWCNTs. The kink model can be used to improve the permeability by changing the diameter of the SWCNTs, while keeping a high selectivity in the gas separation process. The most important is that it is very convenient to obtain the required purity of the oxygen and permeability by adjusting the bending angle of SWCNTs.

DOI: [10.1103/PhysRevB.78.035439](https://doi.org/10.1103/PhysRevB.78.035439)

PACS number(s): 61.46.Fg, 02.70.Ns, 66.90.+r

I. INTRODUCTION

Single-walled carbon nanotubes (SWCNTs) have many potential applications such as molecular sieving, membranes, sensors, and nanopipe for the delivery of gases or liquids.¹⁻⁷ Usually, the effectiveness of molecular sieving is bounded by a tradeoff between selectivity and permeability with higher permeability resulting in lower selectivity. SWCNTs offer the possibility of improving the selectivity bound as they exhibit significantly higher fluxes than other membrane materials, as shown by Skoulidas *et al.*⁸ They found that transport rates of the light gases in carbon nanotubes are orders of magnitude faster than in the zeolites. Then, Majumder *et al.*⁹ found that liquid flow through a membrane composed of an array of aligned carbon nanotubes is four to five orders of magnitude faster than what would be predicted from the conventional fluid-flow theory. The reason is that axial smoothness of the interaction of the molecules with the carbon nanotube walls results in large transport diffusion coefficients. For the same reason, Holt *et al.*¹⁰ discovered that microfabricated membranes, in which aligned carbon nanotubes with diameters of less than 2 nm, which serve as pores have permeabilities more than an order of magnitude larger than the current commercial polycarbonate membranes when gas and water flow pass through them. All of these results suggest that carbon nanotubes could be used to synthesize membranes with both high selectivity and high fluxes to overcome the limitation in current membranes. Accordingly, research on SWCNTs has identified them as a possible material for separation membranes.

On the basis of the research mentioned above, gas separation using carbon nanotubes has attracted considerable attention in recent years. Since the nitrogen adsorption energy was found to increase as the nanotube diameter was reduced toward the molecular diameter of nitrogen,¹¹ many papers appeared characterizing such hypothetical nanotube-based membrane. Separation of a nitrogen-oxygen mixture by SWCNTs was studied by Arora and Sandler¹² using grand canonical Monte Carlo simulations at a range of nanotube diameters, temperatures, and pressures. Their work focuses on SWCNTs to facilitate the rational design of nanomem-

branes for the optimal separation of nitrogen and oxygen from the air. They found that the adsorptive selectivity of a mixture depends strongly on the nanotube diameter, temperature, and structural organization of the adsorbate molecules inside a nanotube. They also studied the mass transport of pure nitrogen, pure oxygen, and their mixture in SWCNTs using molecular dynamics simulations.¹³ High permeability has been observed for both pure components and the mixture inside the nanotubes. It is demonstrated that a good kinetic selectivity can be achieved for air separation using SWCNTs by adjusting the upstream and downstream pressures. Then, they found that tailored carbon nanotubes with constrictions can also exhibit molecular sieving, and therefore it is possible to design more efficient membranes with both high selectivity and mass transport.¹⁴ Although these simulations provide an understanding of the mechanism for the separation of similarly sized gas molecules using nanoporous carbon materials, there is continuing interest in identifying molecular sieving materials and devices with even better selectivity and permeability. In this research, a more efficient model to perform gas separation by the kink of SWCNTs is proposed and studied using molecular dynamics simulations. The results show that the kink model can also achieve the separation of similarly sized gas molecules (N_2 and O_2) and can be used to improve the permeability by changing the diameter of the SWCNTs, while keeping high selectivity in the gas separation process.

II. MODEL AND METHODS

An armchair-type SWCNT_n [which means (n,n) SWCNT] of a total length of 20.2 nm is equilibrated using the equilibrium molecular dynamics (EMD) method in the canonical ensemble (NVT) with the Nosé-Hoover thermostat.¹¹ Equilibration is achieved by coupling the gas to a fixed temperature thermostat at 300 K. Then, a single kink is formed by rotating (bending) the atoms at the right end of the tube, while keeping the left segment of 7 nm as rigid. After that, the gas is inserted into the tube on the left side of the kink and the whole system is equilibrated for 0.1 ns. Finally, the gas molecules are pushed toward the kink by a

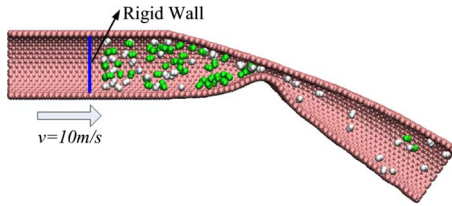


FIG. 1. (Color online) Snapshot of the mixed nitrogen and oxygen passing through the kink of a SWCNT20 at 0.75 ns, in which white and green (dark gray) molecules are oxygen and nitrogen, respectively, and only a half of the tube is shown for clarity.

rigid wall, which reflects the particles attempting to move through it as depicted in Fig. 1. The rigid wall shifts at a constant velocity until it moves at 6 nm from the left end of the tube. The simulations in the last stage are also carried out in the canonical ensemble, and the tubes are treated as rigid bodies for computational efficiency. The Verlet-neighbor list method is implemented to speed up the simulations. A cutoff of 13 Å is used to truncate the adsorbate-adsorbate and adsorbate-adsorbent interactions. The adsorbate-adsorbate and adsorbate-adsorbent interactions are described using a Lennard-Jones 6–12 potential, $U_{LJ}(r) = 4\epsilon[(\sigma/r)^{12} - (\sigma/r)^6]$, where σ and ϵ are the potential parameters, and r is the separation distance between sites i and j . The gas-carbon interaction parameters used were obtained by Bojan and Steele^{15,16} by fitting low-coverage adsorption data of nitrogen and oxygen on planar graphite sheets. The gas-gas interaction parameters for nitrogen¹⁷ and oxygen¹⁸ were obtained by fitting experimental bulk properties. Nitrogen and oxygen are treated as flexible molecules, and a harmonic potential is used to model the intermolecular potential $\phi_v(x) = 1/2 K(x - x_e)^2$, where x_e is the equilibrium bond length and K is the harmonic spring constant, which is derived from the experiment.¹⁹ All the intermolecular potential constants used in the present work can be found in Ref. 13.

III. SIMULATION AND RESULTS

First, the separation of the mixed nitrogen and oxygen (53 O₂, 53 N₂) by a SWCNT20 with the bending angle of 38° is considered. The mixture is inserted into the tube space on the left side of the kink, and the system is equilibrated for 0.1 ns. During this period, a thin gas molecule layer attached to the wall of the SWCNT20 is formed, which is similar to that observed by Arora *et al.*¹¹ Then, a rigid wall as described above is moved toward the kink at a constant velocity of 10 m/s (the system is allowed to equilibrate for 0.1 ns followed by a period of 0.1 ns of movement), and the attached layer disappears. On the left side of the kink, the density of molecules close to the kink is larger than other spaces due to the absorption of the kink. A snapshot of the gas separation process at 0.75 ns is shown in Fig. 1 (only a half of the tube is shown for clarity), in which oxygen molecules are the main gas that has passed through the kink of the SWCNT20. The number of gas molecules on the left side of the kink is counted and plotted as a function of the simulation time in Fig. 2. The number of the nitrogen molecules does not change much during the movement of the rigid wall, result-

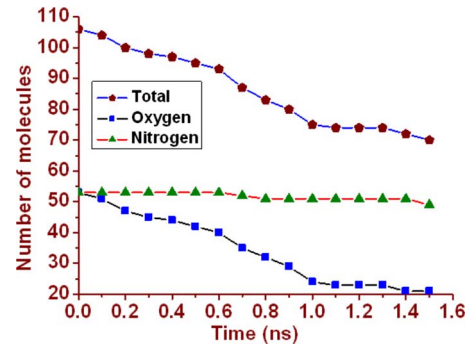


FIG. 2. (Color online) The number of molecules on the left side of the kink in a SWCNT20 as a function of time for a mixed nitrogen and oxygen gas system. The tube has a bending angle of 38°.

ing in the curve of the total gas almost parallel to the curve of oxygen. That is to say, the total number of mixed gas molecules on the left side decreases gradually with time, mainly resulting from the decrease in the number of oxygen molecules. The SWCNT20 with a bending angle of 38° presents a strong selectivity of allowing oxygen over nitrogen to pass through the kink, although these two gases have very similar molecular sizes and interaction energies.

Configurations of pure nitrogen and pure oxygen are generated by inserting 106 molecules into the left side of kinks of SWCNT20. The rigid walls are also moved toward the kinks at a constant velocity of 10 m/s (also equilibrate for 0.1 ns followed by a period of 0.1 ns of movement) after the EMD simulations. For both of the two cases, the simulations are performed under the same conditions. The numbers of O₂ and N₂ molecules on the left side of the kink are plotted as functions of time in Fig. 3. It shows obviously that the number of nitrogen molecules on the left side decreases a little, while nearly a half of the oxygen molecules have passed through the kink, which is very similar from the mixed gas system shown in Fig. 2. This result explains why the kink of the SWCNT20 with a bending angle of 38° can selectively transport oxygen and nitrogen through the tube. However, the permeabilities of oxygen in pure oxygen and mixed gases are different due to the presence of nitrogen molecules. At

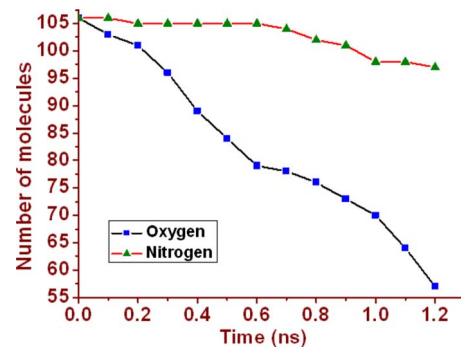


FIG. 3. (Color online) The number of nitrogen and oxygen molecules on the left side of the kinks in SWCNT20 as a function of time for both pure nitrogen and pure oxygen gas systems. The tube has a bending angle of 38°.

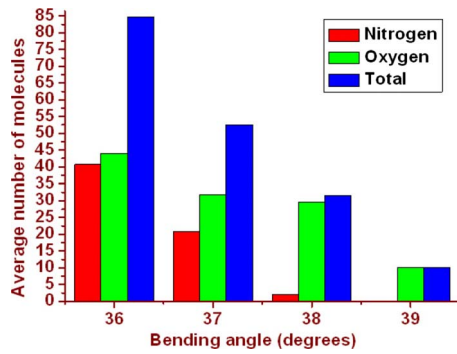


FIG. 4. (Color online) At 1.2 ns, the average numbers of molecules passed through the kinks as functions of the bending angle of a SWCNT20. The averages are computed with five trajectories.

1.2 ns, 50 oxygen molecules can pass through the kink in the case of pure oxygen (106 O_2), while 30 oxygen molecules in the case of the mixture (53 O_2 and 53 N_2). In the pure oxygen system, if we divide the oxygen molecules into two equal groups (53 O_2 and 53 O_2), each group would hold the half of the kink channel because they have the same opportunity to pass through the kink. Then, 25 oxygen molecules of each group can pass through the kink in this system, resulting in a total number of 50 passed molecules, whereas, in the case of the mixture, few nitrogen molecules can pass through the kink, although the two groups have the same number of molecules, implying that the oxygen molecules hold nearly the whole kink channel. Thus, five extra oxygen molecules pass through the kink using the half channel that is supposed to be assigned to nitrogen. Therefore, a total number of 30 oxygen molecules pass through the kink, which is more than the half number of passed oxygen molecules in the pure oxygen case. That is, the permeability of oxygen is enhanced in the mixture.

It is known that the adsorptive selectivity of a mixture depends strongly on the nanotube diameter.¹² In our simulations, the adsorptive selectivity may also depend on the size of kinks. To investigate such an effect, the same EMD simulations for processes of gas molecules passing through different kinks are performed with the same model depicted in Fig. 1. The initial configuration of the N_2/O_2 mixture is also the same as mentioned above. The kink size is changed by changing the bending angle of the SWCNT20. At 1.2 ns, the average numbers of molecules passing through the kinks are obtained as functions of bending angles, as shown in Fig. 4. It can be seen that the total number of molecules passing through the kinks decreases gradually with increasing the bending angle, namely, the permeability is reduced due to the decrease of the kink size. At the bending angle of 36°, the average numbers of the nitrogen and oxygen molecules are nearly equal to each other. From 36° to 37°, both nitrogen and oxygen molecules passing through the kinks decrease largely with the decrease of the kink size. From 37° to 38°, the nitrogen molecules passing through the kinks decrease further, while the permeability of oxygen molecules keeps nearly the same as in the previous case. The reason is that the molecules passing through the kink have an obstructive effect on each other. At the bending angle of 38°, only two

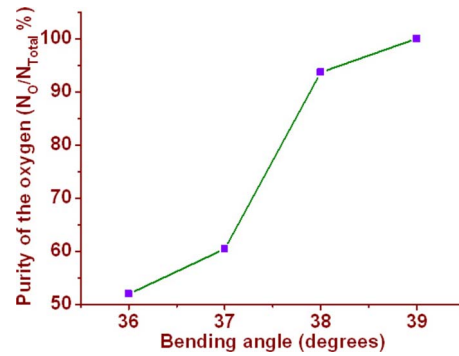


FIG. 5. (Color online) The purity of the oxygen N_O/N_{Total} , where N_O , and N_{Total} are the average numbers of the nitrogen and the total molecules passed through the kink, respectively, as a function of the bending angle of a SWCNT20.

nitrogen molecules can pass through the kink, which results in a smaller obstructive effect on the oxygen molecules. Thus, the number of oxygen molecules passing through the kink has nearly no decrease from the bending angles of 37° to 38°. When the bending angle is 39°, there are only ten oxygen molecules and no nitrogen can pass through the kink. As the bending angle of the SWCNT20 is increased to 40°, neither of nitrogen and oxygen molecules can be found on the right side of the kink. It means that the bending angle of 39° for the SWCNT20 is a threshold above, which nitrogen molecules cannot pass through the kink, while the bending angle of 40° is the threshold for oxygen. This difference is mainly attributed to the slight difference in molecular size between, and is also the different molecules dominant factor for gas separation.

The purity of oxygen after separation, which is the ratio of the average number of oxygen molecules to the average number of total molecules passing through the kink, can be obtained as a function of the bending angle of the SWCNT20, as shown in Fig. 5. It can be easily found that the purity of oxygen increases with the increase in the bending angle. The effectiveness of separation is not obvious at the angle of 36°, while the purity of oxygen improves dramatically from 37° to 38°. At the bending angle of 39°, the kink just permits the oxygen molecules to pass through the SWCNT20. It is known that the effectiveness of separation is bounded by a tradeoff between selectivity and permeability.¹² Based on the linear weighting method, a sieve factor W , $W = \alpha C + (1 - \alpha)Q/Q_0$ ($\alpha = 0.6$) is used to evaluate the tradeoff, where C represents the purity of the oxygen after separation, Q is the number of the oxygen molecules passing through the kink, and Q_0 is the total number of the oxygen molecules. Figure 6 plots the sieve factor W as a function of the bending angle. It shows clearly that the maximum of the sieve factor occurs at the bending angle of 38°. The selectivity at the bending angle of 39° is a little better than that at the bending angle of 38°, whereas the permeability of oxygen is much larger in the latter case. Namely, the bending angle of 38° is the most favorable that make an appropriate kink size for the SWCNT20 to separate the N_2 and O_2 mixture. The effect of a SWCNT10 with a kink on the gas separation is also studied, and the bending

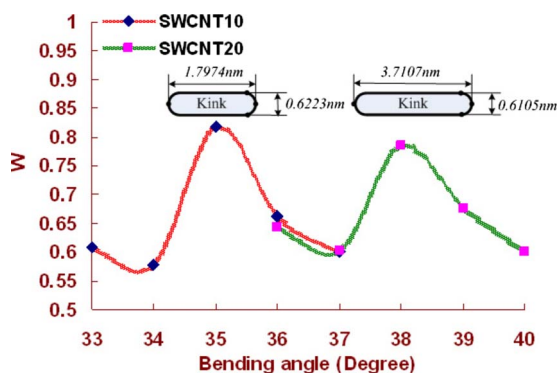


FIG. 6. (Color online) The sieve factors as functions of the bending angles of SWCNT20 and SWCNT10.

angle of 35° is found to be optimal for the separation of N_2 and O_2 is shown in Fig. 6. By comparing kink shapes and sizes between these two SWCNTs with their optimal bending angles, it can be found that these kinks can be simplified as slit shaped pores,²⁰ and the slit widths are very close to each other in both cases, namely, 0.6105 and 0.6223 nm in the case of the SWCNT20 with the bending angle of 38° , and in the case of the SWCNT10 with the bending angle of 35° , respectively. The similar slit width of kinks results in nearly the same selectivity.²¹ However, it should be noted that the permeability in the SWCNT20 is higher than in the SWCNT10, since the cross-section area of the former is larger than that of the latter. These observations can be used to improve the permeability, while keeping a high selectivity in a gas separation process.

To investigate the effect of the velocity of the rigid wall on the gas separation process, the average numbers of molecules passing through the kink are computed when the rigid wall moves 6 nm continuously from the left end of the SWCNT20 at different velocities, as shown in Fig. 7. The total number of molecules passing through the kink decreases with increasing the velocity of the rigid wall. There is a measurable difference between the curves for nitrogen and oxygen, and the effect of the velocity of the rigid wall in the decrease in the number of oxygen is much larger than in the decrease in the number of nitrogen. However, the purity of oxygen after separation is influenced a little by the velocity of the rigid wall, which is about 90% with small fluctuations. That is, the velocity of the rigid wall can influence the numbers of molecules passing through the kink, while it is independent of the selectivity in the gas separation process.

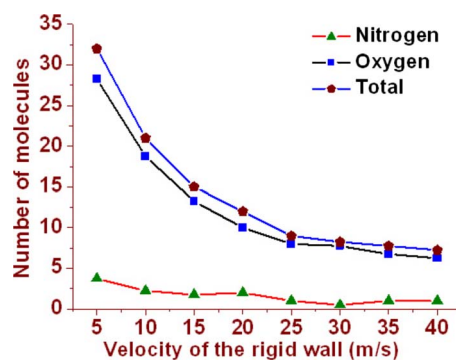


FIG. 7. (Color online) The average numbers of molecules passing through the kink as functions of the velocity of the rigid wall when it moves 6 nm continuously from the left end of a SWCNT20.

IV. CONCLUSIONS

In summary, molecular dynamics simulations have been conducted to study the transport of pure nitrogen, oxygen, and their mixture in a SWCNT20 with a kink. The permeability of gases decreases, while the selectivity of the tube increases with increasing the bending angle of a SWCNT20. Although there is a very small difference in the molecular sizes of nitrogen and oxygen, the SWCNT20 with the bending angle of 38° has a very high sieving resistance for nitrogen but not for oxygen, resulting in a high selectivity for oxygen. Moreover, the remaining nitrogen at the left side of the kink can be taken out by decreasing the bending angle after oxygen molecules pass through the kink. By using the presented kink model, it is very convenient to obtain the required purity of oxygen by adjusting the bending angle of SWCNTs. The most important is that the permeability of oxygen can also be improved by enlarging the diameter of SWCNTs while keeping a high purity. This result breaches a limit, which is a tradeoff between selectivity and permeability with a higher permeability resulting in lower selectivity. The kink model provides a prototype for many other potential applications, e.g., water desalination, and should be interesting for many researchers in structural material, nanotube, and/or microflow communities and industries.

ACKNOWLEDGMENTS

The supports of the National Natural Science Foundation of China Grant Nos. 10721062, 90715037, 50679013 and 10640420176, the Program for Changjiang Scholars and Innovative Research Team in University of China (PCSIRT), the 111 Project (No. B08014) and the National Key Basic Research Special Foundation of China (2005 CB321704) are gratefully acknowledged.

*zhanghw@dlut.edu.cn

¹G. Hummer, J. C. Rasaiah, and J. P. Noworyt, *Nature (London)* **414**, 188 (2001).

²R. Q. Long and R. T. Yang, *J. Am. Chem. Soc.* **123**, 2058 (2001).

³L. Sun and R. M. Crooks, *J. Am. Chem. Soc.* **122**, 12340 (2000).

⁴S. A. Miller, V. Y. Young, and C. R. Martin, *J. Am. Chem. Soc.* **123**, 12335 (2001).

⁵Z. F. Ren, Z. P. Huang, J. W. Xu, J. H. Wang, P. Bush, M. P. Siegal, and P. N. Provencio, *Science* **282**, 1105 (1998).

⁶T. D. Power, A. I. Skoulidas, and D. S. Sholl, *J. Am. Chem. Soc.* **124**, 1858 (2002).

- ⁷Q. Wang, S. R. Challa, D. S. Sholl, and J. K. Johnson, *Phys. Rev. Lett.* **82**, 956 (1999).
- ⁸A. I. Skoulidas, D. M. Ackerman, J. K. Johnson, and D. S. Sholl, *Phys. Rev. Lett.* **89**, 185901 (2002).
- ⁹M. Majumder, N. Chopra, R. Andrews, and B. J. Hinds, *Nature (London)* **438**, 44 (2005).
- ¹⁰J. K. Holt, H. G. Park, Y. Wang, M. Stadermann, A. B. Artyukhin, C. P. Grigoropoulos, A. Noy, and O. Bakajin, *Science* **312**, 1034 (2006).
- ¹¹G. Arora, N. J. Wagner, and S. I. Sandler, *Langmuir* **20**, 6268 (2004).
- ¹²G. Arora and S. I. Sandler, *J. Chem. Phys.* **123**, 044705 (2005).
- ¹³G. Arora and S. I. Sandler, *J. Chem. Phys.* **124**, 084702 (2006).
- ¹⁴G. Arora and S. I. Sandler, *Nano Lett.* **7**, 565 (2007).
- ¹⁵M. J. Bojan and W. A. Steele, *Langmuir* **3**, 116 (1987).
- ¹⁶M. J. Bojan and W. A. Steele, *Langmuir* **3**, 1123 (1987).
- ¹⁷C. S. Murthy, K. Singer, M. L. Klein, and I. R. McDonald, *Mol. Phys.* **41**, 1387 (1980).
- ¹⁸M. L. Klein, D. Levesque, and J. J. Weis, *Phys. Rev. B* **21**, 5785 (1980).
- ¹⁹D. R. Lide, *CRC Handbook of Chemistry and Physics*, 81th ed. (CRC, Boca Raton, FL, 2000).
- ²⁰M. Grujicic, G. Cao, and W. N. Roy, *Appl. Surf. Sci.* **246**, 149 (2005).
- ²¹A. Singh and W. J. Koros, *Ind. Eng. Chem. Res.* **35**, 1231 (1996).